Coherent Response of Hydrogen Bonds in Liquids Probed by Ultrafast Vibrational Spectroscopy

Jens Stenger,[†] Dorte Madsen,[‡] Jens Dreyer,[†] Erik T. J. Nibbering,[†] Peter Hamm,[†] and Thomas Elsaesser[†]

Max-Born-Institut für Nichtlineare Optik und Kurzzeitspektroskopie, Max-Born-Strasse 2A, D-12489 Berlin, Germany, and Department of Chemistry, Aarhus University, Langelandsgade 140, 8000 Aarhus C, Denmark

Received: August 31, 2000; In Final Form: February 5, 2001

We report the first observation of coherent vibrational dynamics in a hydrogen bond obtained by femtosecond nonlinear measurements in the mid-infrared spectral range. The results provide the first experimental evidence in the time domain for the anharmonic coupling of slow and fast vibrational motions in a hydrogen bond. We show that the absorption band of the high-frequency hydrogen stretching (O−H/O−D) vibration is modulated by a coherent oscillatory motion corresponding to a periodic variation of the hydrogen bond length and its strength. This mechanism, which is of general relevance for hydrogen bonds, is connected with underdamped low-frequency vibrations—in contrast to the assumption of overdamped nuclear motions in most theoretical treatments.

Introduction

Hydrogen bonding determines the structural and functional properties of numerous molecular systems, as coupling of a hydrogen atom to different functional groups establishes a weak chemical bond. Formation of such a bond strongly affects the positions and microscopic motions of the participating nuclei. So far, the mechanisms governing nuclear motions in a hydrogen bond have not been resolved, mainly because of the structural complexity and flexibility of hydrogen-bonded liquids such as water and of biological systems.

The high-frequency vibrational stretching band of the X−H group in a X−H···Y hydrogen bond changes strongly upon hydrogen bonding, the most evident effects being the red-shift of the ν(X−H) frequency compared to a free X−H group, its intensity increase and broadening, often accompanied by a peculiar band shape with substructure. Hydrogen bonding leads to a dramatic distortion of the potential energy surfaces that determine the nuclear positions and motions, giving rise to strongly anharmonic or even double-well potentials.[1] Theoretical models suggest that the enhanced anharmonicity of the potential energy surfaces results in a coupling of the X−H stretching mode at high frequency and of low-frequency modes, which change the X···Y distance.[1−7] The strong broadening of the X−H stretching band has been attributed to the formation of vibrational sidebands, consisting of a X−H stretching excitation plus/minus quanta of the low-frequency mode. The additional broadening occurring in liquids has been ascribed to the interaction of hydrogen bonds with the fluctuating solvent, leading to dephasing of the high-frequency mode and damping of the low-frequency motion. These effects have been described by quantum mechanical treatments of interaction[2] as well as classical Brownian oscillator models for the low-frequency mode.[6] Previous experimental studies of ultrafast vibrational dynamics have concentrated on incoherent relaxation and energy transfer processes in hydrogen-bonded liquids, without, however, addressing vibrational motions and anharmonic coupling directly.[8−11]

As the structural complexity and flexibility of hydrogen-bonded systems in the condensed phase is very high and cannot be resolved spectroscopically, specific insight into such phenomena can be obtained only from model systems displaying a well-defined hydrogen-bonding geometry and the characteristic vibrational line shapes. We therefore study phthalic acid monomethylester (PMME, Figure 1a) in the nonpolar solvent C_2Cl_4 as a prototypical example of a medium strong intramolecular hydrogen bond. To eliminate the interference of C−H stretching modes within the high-frequency band, our study is focused on the O−D stretching band of the carboxy-deuterated derivative (PMME-D). Its stationary infrared spectrum shown in Figure 1b exhibits the typical features, such as strong red-shift and broadening of the band and the appearance of (in this case) two main subbands, predicted by the above-mentioned theoretical treatments. A quantitative understanding of such highly complex bands has not been reached so far. In particular, the coupling of slow and fast vibrational motions cannot be derived from the stationary spectra. In contrast, nonlinear ultrafast IR spectroscopy monitors transmission changes of the high-frequency O−D band and thus provides direct access to observe vibrational motions of the hydrogen bond in real time.

Experimental Section

Femtosecond IR pump−probe experiments were performed with mid-infrared pulses of 130 fs duration, 150 cm^{-1} bandwidth, and more than 1 μJ energy/pulse at a 1 kHz repetition rate produced by parametric difference frequency mixing in $AgGaS_2$.[12] The intense pump pulse induces in the sample nonlinear transmission changes that are monitored by time delayed probe pulses. The probe pulse is spectrally dispersed after interaction with the sample and broad-band detected by a 16-channel HgCdTe detector. PMME-D was prepared by shaking a solution of PMME in C_2Cl_4 (30 mM) with D_2O and

[†] Max-Born-Institut.
[‡] Aarhus University.

10.1021/jp003153h CCC: $20.00
Published on Web 03/13/2001

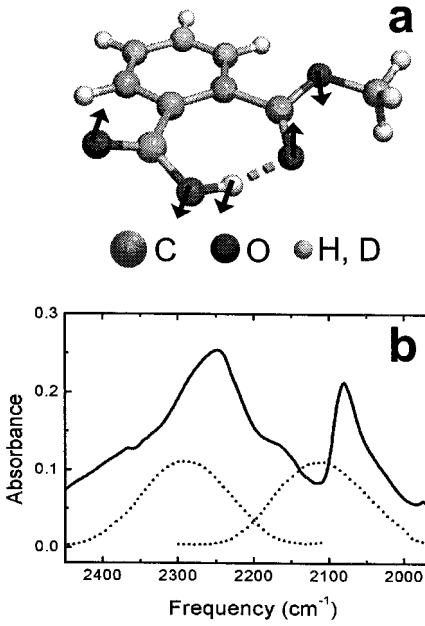

Figure 1. (a) Molecular structure of PMME-D (2-DOOC$-C_6H_4-$COOCH$_3$). Arrows denote the normal coordinate of the low-frequency mode calculated at 70 cm^{-1} that strongly modulates the H-bond distance. This mode is assigned to the low-frequency motion, which is anharmonically coupled to the high-frequency ν(O−D) mode. (b) Linear O−D stretching absorption spectrum (solid line) and power spectra of the pump and probe pulses (dashed line).

subsequent separation of the organic phase (sample thickness: 0.5 mm).

Results and Discussion

We performed two series of measurements with pulses centered at 2100 and 2300 cm^{-1} (Figure 1b). In Figure 2a, the change of absorption as a function of delay time and probe frequency is shown for excitation and probe pulses centered at 2300 cm^{-1}. Individual transients are plotted in Figure 2b for probe frequencies of 2315, 2271, and 2213 cm^{-1}. Depending on the probe frequency, induced absorption or bleaching occur, superimposed by pronounced oscillations for positive delay times.[13] A similar behavior is found with excitation and probe centered at 2100 cm^{-1}, as is shown in Figure 2b displaying the time evolution of enhanced absorption at 2028 cm^{-1}. It is important to note that the period of the oscillatory signals is identical in all measurements. Furthermore, a phase shift of the oscillations of 180° is observed in going from the red (2213 cm^{-1}) to the blue side (2315 cm^{-1}) of the data set (Figure 2a,b). At intermediate frequency positions the oscillation amplitude vanishes (cf. the transient at 2271 cm^{-1}, Figure 2b).

We use singular value decomposition (SVD), a standard numerical procedure, to extract uncorrelated components from the data set in Figure 2a, which consists of mutually dependent time-frequency traces.[15] Each resulting component is characterized by a spectral amplitude, a temporal evolution, and a singular value, the size of which determines its significance. The orthonormal basis set obtained is then transformed by linear combination to create physically meaningful basis functions. The application of this procedure reduces the experimental data to only two major components whose time evolutions are displayed in Figure 3a,b with their spectral representation given as insets. The first SVD component (Figure 3a, solid line) shows a fast monoexponential decay with a time constant of ∼400 fs superimposed by very weak oscillations. This component of negative amplitude represents a decrease of absorption

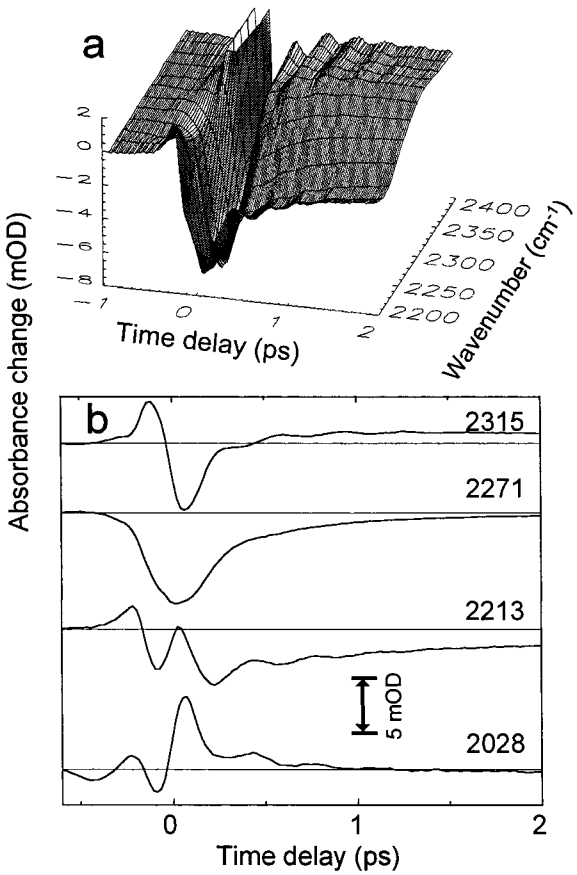

Figure 2. (a) Nonlinear change $\Delta A = -\log(T/T_0)$ of vibrational absorbance of PMME as a function of pump−probe delay and probe frequency (T_0,T: transmission of the sample before and after excitation centered at 2300 cm^{-1}). Positive signals correspond to enhanced absorption, negative signals to bleaching. (b) Time-resolved absorbance change at probe frequencies of 2315, 2271, 2213 cm^{-1} (excitation centered at 2300 cm^{-1}), and 2028 cm^{-1} (excitation centered at 2100 cm^{-1}).

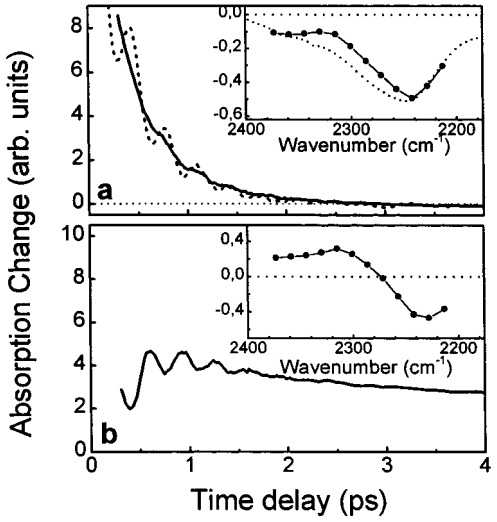

Figure 3. Temporal evolution (solid lines) and spectra (insets) of the two dominant components obtained from singular value decomposition of the temporally and spectrally resolved data in Figure 2a. (a: dashed line: Time-resolved absorbance change for positive delay times at a probe frequency of 2028 cm^{-1}, excitation pulse centered at 2100 cm^{-1}).

with a spectrum (Figure 3a, inset, solid line) similar to the ν(O−D) absorption spectrum (Figure 3a, inset, dashed line). The second SVD component (Figure 3b) displays two correlated contributions, strong oscillations persisting up to ∼1.5

ps and slow relaxation on a time scale of ~20 ps. The spectral representation (Figure 3b, inset) exhibits the signature of a first derivative of the ν(O−D) ground-state absorption band with respect to frequency.

The decay of the first SVD component may be compared to the time trace that is found at 2028 cm^{-1} and displays an enhanced absorption (Figure 2b and dashed line in Figure 3a). At this spectral position, essentially no ground-state absorption remains, so that the signal can be safely attributed to the anharmonically red-shifted transition from the $v_{OD} = 1$ to the $v_{OD} = 2$ level.[8−11] The oscillations in this signal demonstrate vibrational wave packet motion in the $v_{OD} = 1$ state. The very good agreement of the two decays confirms that the fast SVD component (excitation at 2300 cm^{-1}) originates from molecules in the first excited vibrational state ($v_{OD} = 1$) and decays by population relaxation with a vibrational lifetime of $T_1 \sim 400$ fs. Its spectral amplitude of negative sign is thus interpreted as the sum of contributions from bleaching (transition from $v_{OD} = 0$ to $v_{OD} = 1$) and stimulated emission (transition from $v_{OD} = 1$ to $v_{OD} = 0$) both having a shape close to the ground-state absorption band.

The incoherent long time decay observed in the second SVD component can be attributed to incoherent excitation of low-frequency modes through energy dissipation and relaxation in vibrationally excited molecules, giving rise to a blue-shift at longer times. Such molecules relax back to equilibrium on a 10 to 30 ps time scale, as has been discussed previously for intermolecular H-bonds.[16]

The striking feature of this study is the observation of pronounced coherent oscillations in the second SVD component. As is evident from the spectrum (Figure 3b, inset), this SVD component represents an increase of absorption at higher frequencies and a decrease at lower frequencies. Such a frequency shift is a measure for the H-bond strength and corresponds to a weakening of the H-bond, i.e., an increase of the average oxygen−oxygen distance in the hydrogen bond. The oscillatory behavior up to delay times of about 1.5 ps reflects a periodic modulation of this distance by a coherent vibrational motion of low frequency which is initiated by the pump pulse. This interpretation is supported by the observed phase shift of the oscillations of 180° between the red (2213 cm^{-1}) and blue (2315 cm^{-1}) side of the data set (Figure 2a,b) and by the fact that the oscillation amplitude vanishes at intermediate frequencies (2271 cm^{-1}), i.e., around the maximum of the ν(O−D) absorption band. The damping time of the oscillations amounts to 400 fs, which appears to be equal to the lifetime T_1 of the excited vibrational state $v_{OD} = 1$.

Figure 4 a,b schematically depicts potential energy curves for the high-frequency O−D stretching mode, assuming a decrease of the equilibrium hydrogen bond length in the $v_{OD} = 1$ state, into which the vibrational levels v_{HB} of the low-frequency mode modulating the hydrogen bond length are drawn. Excitation of the $v_{OD} = 1$ level by the pump pulse creates a nonstationary coherent superposition of anharmonically coupled low-frequency states (v_{HB}) within the pump bandwidth, giving rise to the oscillations in the excited vibrational state (Figure 4a). The wave packet initially moves to probe frequencies on the red side of the pulse. Equally likely, a coherent superposition of low-frequency states (v_{HB}) in the $v_{OD} = 0$ state is generated through an impulsive Raman process within the pump bandwidth (Figure 4b). There might be an additional contribution caused by molecules initially promoted to the $v_{OD} = 1$ state that preserve vibrational coherence even after relaxation back to the $v_{OD} = 0$ state and thus contribute to coherent motion.

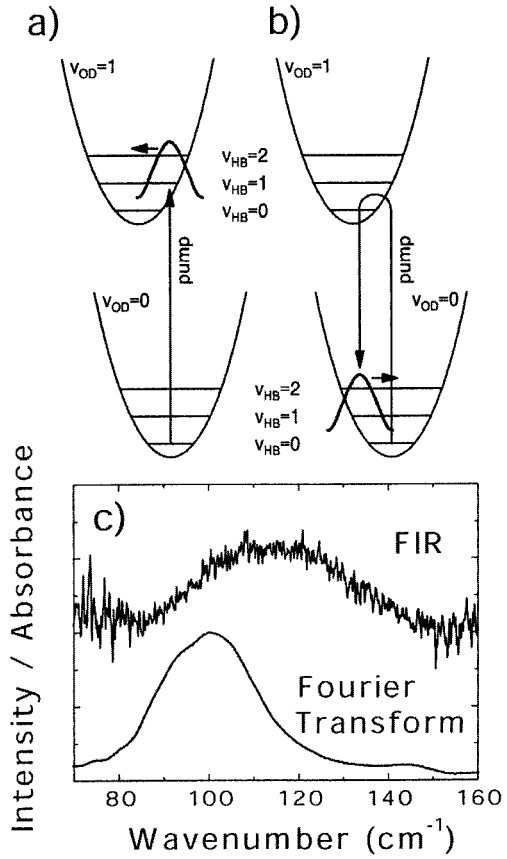

Figure 4. Schematic potential energy curves for the O−D stretching mode assuming an origin shift of the $v_{OD} = 1$ curve to smaller hydrogen bond length with wave packets created by the pump pulse (a) in the excited vibrational state $v_{OD} = 1$ and (b) in the vibrational ground state ($v_{OD} = 1$) through an impulsive Raman process. Vibrational levels of the low-frequency mode that modulates the hydrogen bond length are denoted by v_{HB}. Arrows signify the direction of the initial momentum of the wave packets. (c) Fourier transform of the second SVD component, together with the far-infrared (FIR) vibrational absorption spectrum of PMME-D.

Both absorption of the ground-state wave packet (Figure 4b) and stimulated emission from the excited vibrational wave packet (Figure 4a)—the latter contributing with a negative sign—exhibit the signature of an oscillating ν(O−D) absorption band (Figure 3b, inset). Thus, molecules in the $v_{OD} = 0$ and $v_{OD} = 1$ states may contribute to the coherent signal shown in the second SVD component.

The occurrence of coherent oscillatory motions in both the $v_{OD} = 0$ and the $v_{OD} = 1$ state clearly demonstrates a pronounced anharmonic coupling between the high-frequency O−D stretching vibration and low-frequency modes. The persistence of coherent low-frequency oscillations up to delay times of about 1.5 ps contrast the assumption of overdamped nuclear motions made in most theoretical treatments of hydrogen bonds in the condensed phase.[1,2,6]

To investigate the nature of the anharmonically coupled low-frequency motion, we present a Fourier analysis of the time-resolved oscillatory signal from the second (slow) SVD component (Figure 4c). The spectrum shows a single maximum at 100 cm^{-1} with a total spectral width of ~25 cm^{-1}. It is important to note that the same spectrum of the oscillatory signal is observed for PMME-H, the protonated compound. The spectrum of the oscillatory signal displays substantial overlap

with the broad and structureless absorption band between 80 and 150 cm^{-1}, which is observed in the steady-state far-infrared spectrum of PMME (Figure 4c). As is known from THz and optical Kerr studies of liquids, both intramolecular and solvent modes contribute to absorption bands in this spectral range, such that the spectral width of the steady-state band cannot be related to purely intramolecular dynamics.[17]

To get insight into the relevant vibrational degrees of freedom, normal mode calculations on PMME-D were performed using density functional theory.[18] The agreement of experimental and theoretical data above 1000 cm^{-1} (not shown) is most satisfactory. This gives confidence for the assignment of low-frequency modes which is, however, known to be more difficult because of the more delocalized character of these modes. Below 150 cm^{-1}, a total number of five normal modes was calculated, all of them being weakly infrared active. The upper two modes correspond to methyl torsions, and the lower three represent out-of-plane motions of the substituents. However, only one of them, calculated to 70 cm^{-1}, affects the geometry of the hydrogen bond in a way indicated by arrows in Figure 1a. The mode is characterized as opposite phase out-of-plane torsional motion of the adjacent ring substituents, a motion similar to the low-frequency shear modes that have been reported to be responsible for relaxational and mode-coupling phenomena of H-bonded liquids such as water.[19] We therefore attribute the oscillations observed in the time-resolved experiments to a coherent excitation of this mode in support of theoretical models of hydrogen bonding based on a coupling of the fast X−H stretching and the slow X···Y motion. This assignment is supported by the concurring experimental and theoretical result that there is no H/D isotope effect for the frequency of this mode. Additional modes with frequencies above ∼250 cm^{-1}, which cannot be resolved with the current time resolution of the experiment, may couple to the high-frequency motion, thereby contributing to the complex vibrational line shape of the stationary ν(O−D) spectrum.

In conclusion, the results presented here emphasize that nonlinear vibrational spectroscopy in the femtosecond time domain can grasp anharmonicity in hydrogen bonds in a much more direct and unambiguous way than does steady-state vibrational spectroscopy. Our experimental finding of anharmonic vibrational coupling in a H-bond will help to refine theoretical models for hydrogen bonding, underlying many fundamental processes in nature.

Acknowledgment. This work is part of the collaborative research center *Analysis and control of ultrafast photoinduced reactions (SFB 450)*, supported by the Deutsche Forschungsgemeinschaft and, in addition, was partially supported by the European Union (HPRI-CT-1999-00084) (D.M.). J.D. gratefully acknowledges a fellowship of the Deutsche Forschungsgemeinschaft. We thank J. Manz, O. Kühn, H. Naundorf, G. K. Paramanov, and N. P. Ernsting for valuable discussions.

References and Notes

(1) *Theoretical Treatments of Hydrogen Bonding*, Hadzi, D., Ed.; John Wiley & Sons: Chichester, 1997.

(2) For a recent review: Henri-Rousseau, O.; Blaise, P. *Adv. Chem. Phys.* **1998**, *103*, 1.

(3) Maréchal, Y.; Witkowski, A. *J. Chem. Phys.* **1968**, *48*, 3697.

(4) Rösch, N.; Ratner, M. A. *J. Chem. Phys.* **1974**, *61*, 3344.

(5) Bratos, S. *J. Chem. Phys.* **1975**, *63*, 3499.

(6) Robertson, G. N.; Yarwood, J. *Chem. Phys.* **1978**, *32*, 267.

(7) Staib, A.; Hynes, J. T. *Chem. Phys. Lett.* **1993**, *204*, 197.

(8) Graener, H.; Seifert, G.; Laubereau, A. *Phys. Rev. Lett.* **1991**, *66*, 2092.

(9) Woutersen, S.; Emmerichs, U.; Bakker, H. J. *Science* **1997**, *278*, 658.

(10) Woutersen, S.; Bakker, H. J. *Nature* **1999**, *402*, 507.

(11) Gale, G. M.; Gallot, G.; Hache, F.; Lascoux, N.; Bratos, S.; Leicknam, J.-Cl. *Phys. Rev. Lett.* **1999**, *82*, 1068.

(12) Hamm, P.; Lim, M.; Hochstrasser, R. M. *J. Chem. Phys.* **1997**, *107*, 10523.

(13) The signal at negative delay times is due to the perturbed free induction decay of the optical polarization induced by the pump pulse and reflects detuning oscillations (see, e.g., ref 14). Around zero delay, the transients are strongly influenced by cross phase modulation, originating mainly from Kerr nonlinearities of the solvent and the CaF_2 windows of the sample cell. Therefore, only values for delay times longer than 300 fs were used for singular value decomposition.

(14) Hamm, P. *Chem. Phys.* **1995**, *200*, 415.

(15) Wise, F.; Rosker, M. J.; Millhauser, G. L.; Tang, C. L. *IEEE J. Quantum Electron.* **1987**, *23*, 1116.

(16) Nienhuys, H.-K.; Woutersen, S.; van Santen, R. A.; Bakker, H. J. *J. Chem. Phys.* **1999**, *111*, 1494.

(17) McMorrow, D.; Thantu, N.; Melinger, J. S.; Kim, S. K.; Lotshaw W. T. *J. Phys. Chem.* **1996**, *100*, 10389.

(18) B3LYP/6-31+G(d,p): Frisch, M. J.; Trucks, G. W.; Schlegel, H. B.; Scuseria, G. E.; Robb, M. A.; Cheeseman, J. R.; Zakrzewski, V. G.; Montgomery, J. A., Jr.; Stratmann, R. E.; Burant, J. C.; Dapprich, S.; Millam, J. M.; Daniels, A. D.; Kudin, K. N.; Strain, M. C.; Farkas, O.; Tomasi, J.; Barone, V.; Cossi, M.; Cammi, R.; Mennucci, B.; Pomelli, C.; Adamo, C.; Clifford, S.; Ochterski, J.; Petersson, G. A.; Ayala, P. Y.; Cui, Q.; Morokuma, K.; Malick, D. K.; Rabuck, A. D.; Raghavachari, K.; Foresman, J. B.; Cioslowski, J.; Ortiz, J. V.; Stefanov, B. B.; Liu, G.; Liashenko, A.; Piskorz, P.; Komaromi, I.; Gomperts, R.; Martin, R. L.; Fox, D. J.; Keith, T.; Al-Laham, M. A.; Peng, C. Y.; Nanayakkara, A.; Gonzalez, C.; Challacombe, M.; Gill, P. M. W.; Johnson, B. G.; Chen, W.; Wong, M. W.; Andres, J. L.; Head-Gordon, M.; Replogle, E. S.; Pople, J. A. *Gaussian 98*; Gaussian, Inc.: Pittsburgh, PA, 1998.

(19) Walrafen, G. E. *J. Phys. Chem.* **1990**, *94*, 2237.